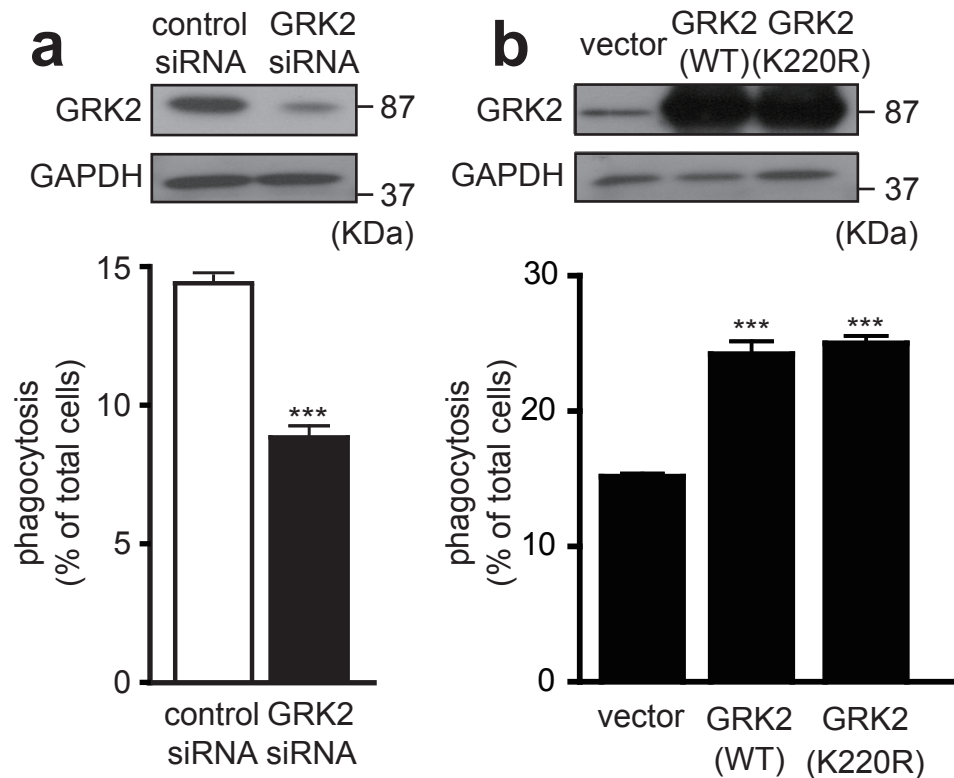
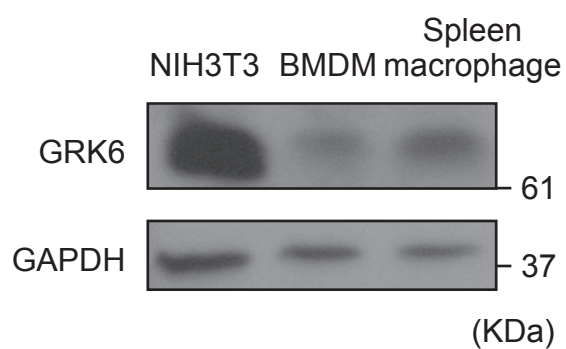


**Supplementary Fig. S1 GRK2 promotes apoptotic engulfment independently of its kinase activity.**



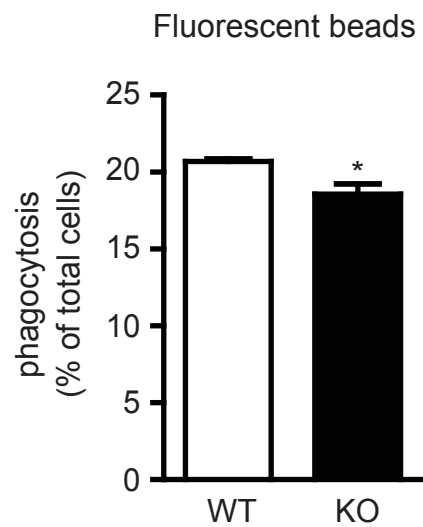
NIH3T3 cells ( $4 \times 10^4$  /well) transfected with siRNA against GRK2 (**a**) or infected with the indicated retroviruses (**b**) in 24-well plate were incubated with fluorescently labeled apoptotic thymocytes ( $1 \times 10^6$  /well) for 90 min at 37 °C. Percentages of the NIH3T3 cells engulfed the apoptotic cells were determined by flow cytometry. All the experiments were done at least three times, and representative data are shown. \*\*\*;  $P < 0.001$ .

**Supplementary Fig. S2 GRK6 expression in NIH3T3 cells, BMDM and splenic macrophages.**



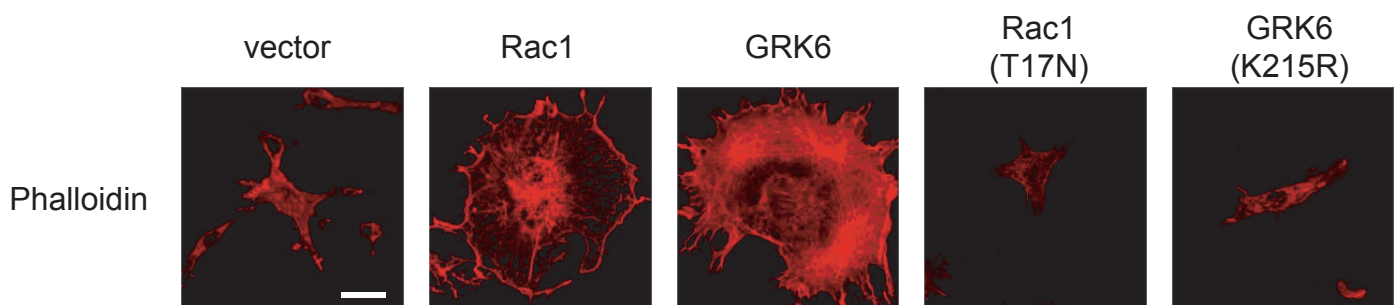
Cell lysates of NIH3T3 cells, BMDM and splenic macrophages were immunoblotted with anti-GRK6 antibody and anti-GAPDH antibody. Representative blots from three independent experiments are shown.

**Supplementary Fig. S3 Engulfment of microspheres by GRK6-deficient BMDM.**



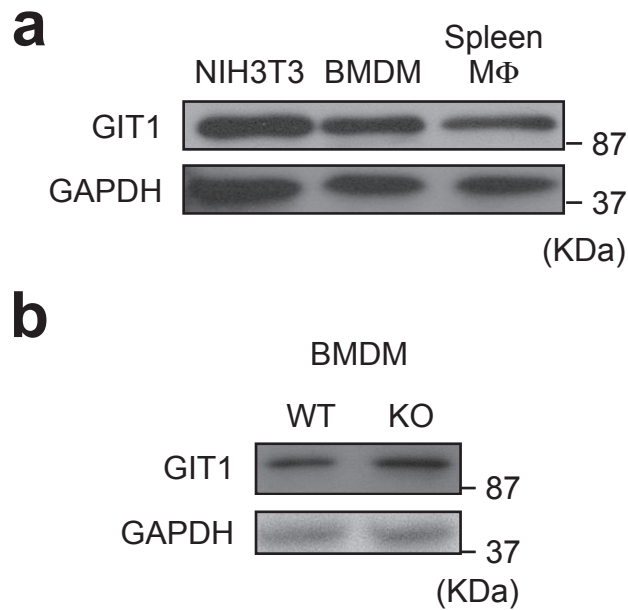
BMDM ( $1 \times 10^5$  /well) from GRK6-deficient mice in 24-well plate were incubated with  $2 \mu\text{m}$  yellow-green fluorescent carboxylate-modified microspheres ( $2.5 \times 10^5$  /well) for 60 min at  $37^\circ\text{C}$ . Percentages of BMDM engulfed the microspheres were determined by flow cytometry. \*;  $P < 0.05$ . Data represent means  $\pm$  s.e.m. (error bars) of three independent experiments.

**Supplementary Fig. S4 GRK6 contributes to the lamellipodia formation in NIH3T3 cells.**



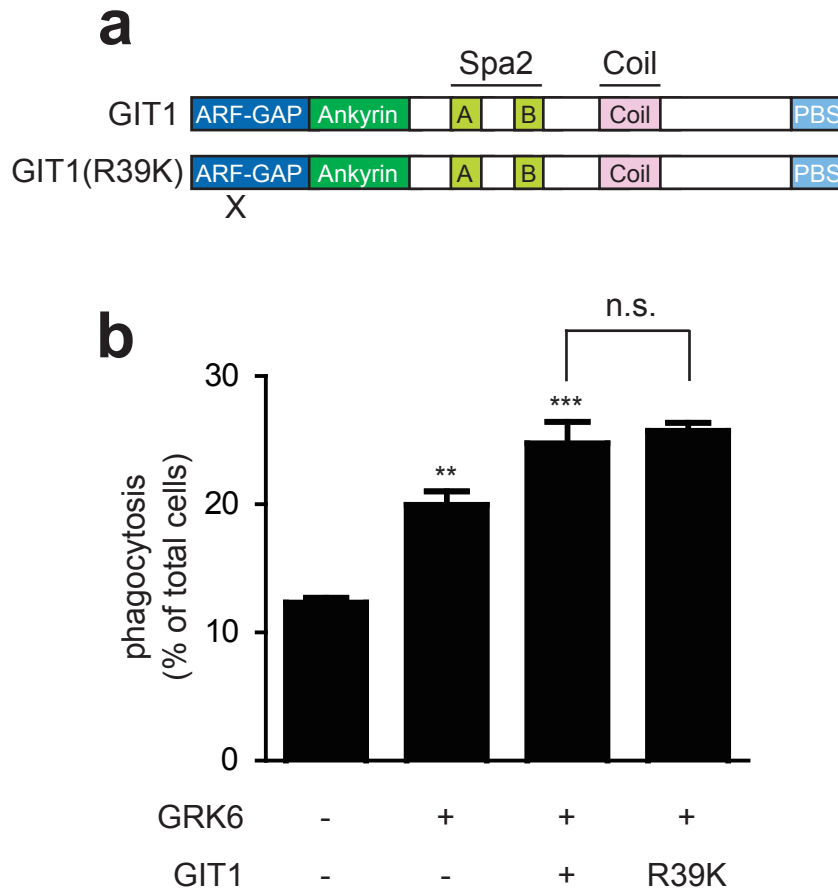
The NIH3T3 cells retrovirally transfected with empty vector, Rac1, GRK6, Rac1 (T17N) or GRK6 (K215R) were fixed and stained with Alexa568-conjugated phalloidin. Scale bar, 20 $\mu$ m.

**Supplementary Fig. S5 GIT1 expression in NIH3T3 cells, BMDM and splenic macrophages.**



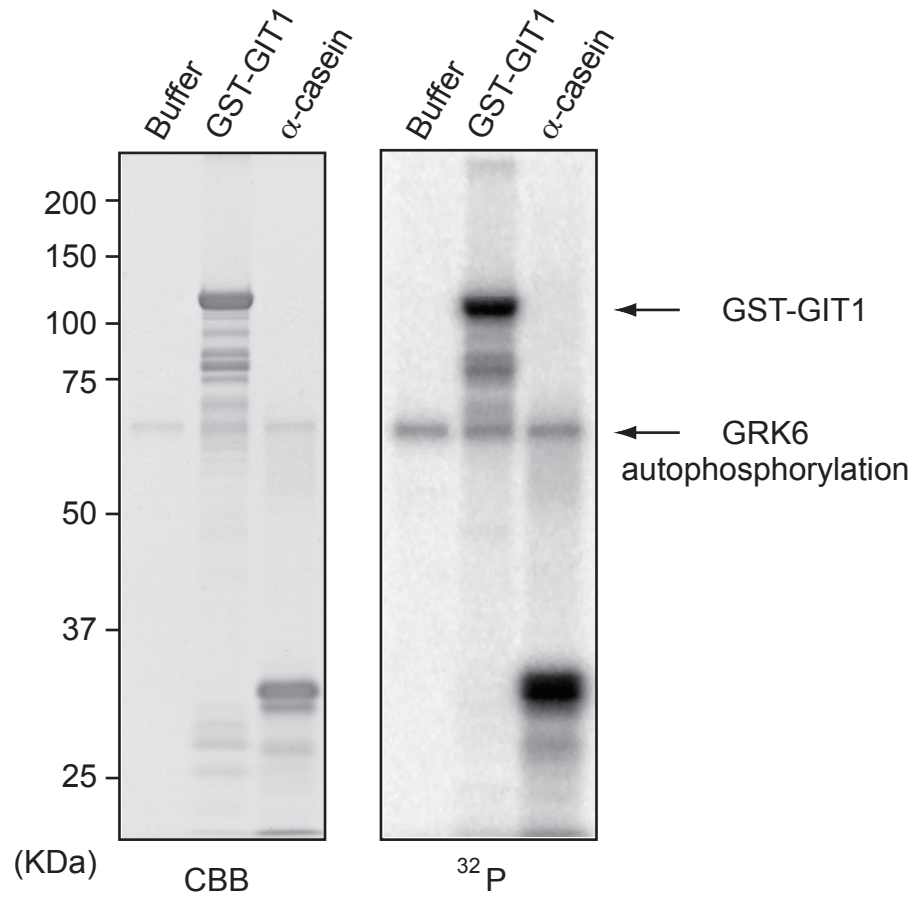
(a) Cell lysates of NIH3T3 cells, BMDM and splenic macrophages were subjected to western blot using anti-GIT1 and anti-GAPDH antibodies. (b) GIT1 expression in BMDM from wild-type and GRK6-deficient mice were detected by western blot using anti-GIT1 antibody. Representative blots from three independent experiments are shown.

**Supplementary Fig. S6 ARF-GAP activity of GIT is not involved in GRK6-mediated engulfment pathway.**



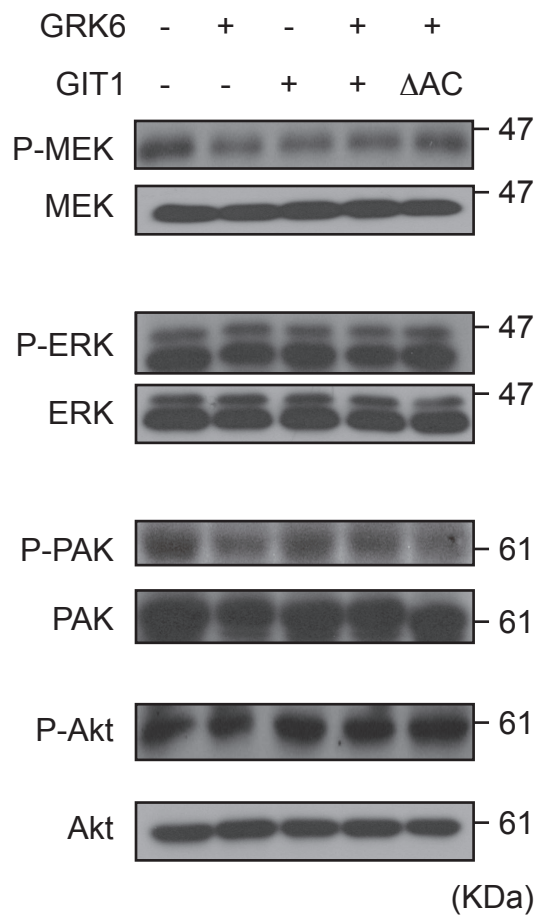
(a) Schematic representation of GIT1 and point mutant of GIT1, GIT1 (R39K) in this study. (b) NIH3T3 cells infected with the indicated retroviruses were subjected to the engulfment assay. Data represent means  $\pm$  s.e.m. (error bars) of four independent experiments. \*\*,  $P < 0.01$ , \*\*\*,  $P < 0.001$ .

**Supplementary Fig. S7 GRK6 directly phosphorylates GIT1.**



GST-fused GIT1 and  $\alpha$ -casein were subjected to *in vitro* kinase assay with GRK6 as detailed in Supplementary Methods. The left gel image represents total protein stained with Coomassie Brilliant Blue, and the right gel image shows autoradiography of  $^{32}\text{P}$  labeling.  $\alpha$ -casein was used as a positive control.

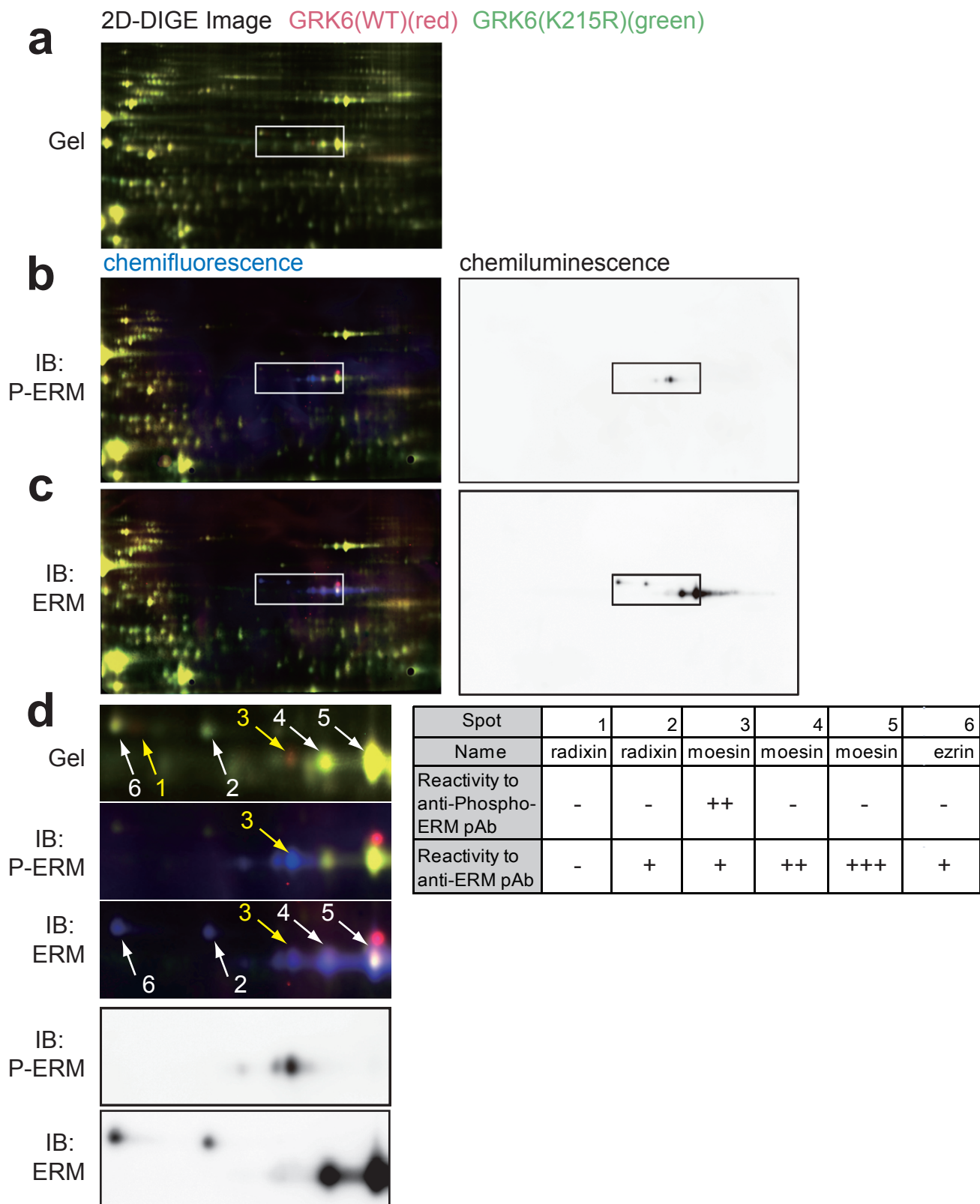
**Supplementary Fig. S8 GRK6/GIT1 complex do not induce Rac1/PAK1/MEK1 activation or Akt phosphorylation.**



Cell lysates of NIH3T3 cells infected with the indicated retroviruses were analyzed by western blot using anti-phospho-MEK1 (Ser298) (1:2000, CST), anti-MEK1 (1:2000, CST), anti-phospho-ERK1/2 (Thr202/Tyr204) (1:5000, CST), anti-phospho-PAK1 (Thr423) (1:2000, CST), anti-PAK1/2/3 (1:5000, CST), anti-phospho-Akt (Ser473) (1:2000, CST) and anti-Akt (1:5000, CST) antibodies. Representative blots from three independent experiments are shown.

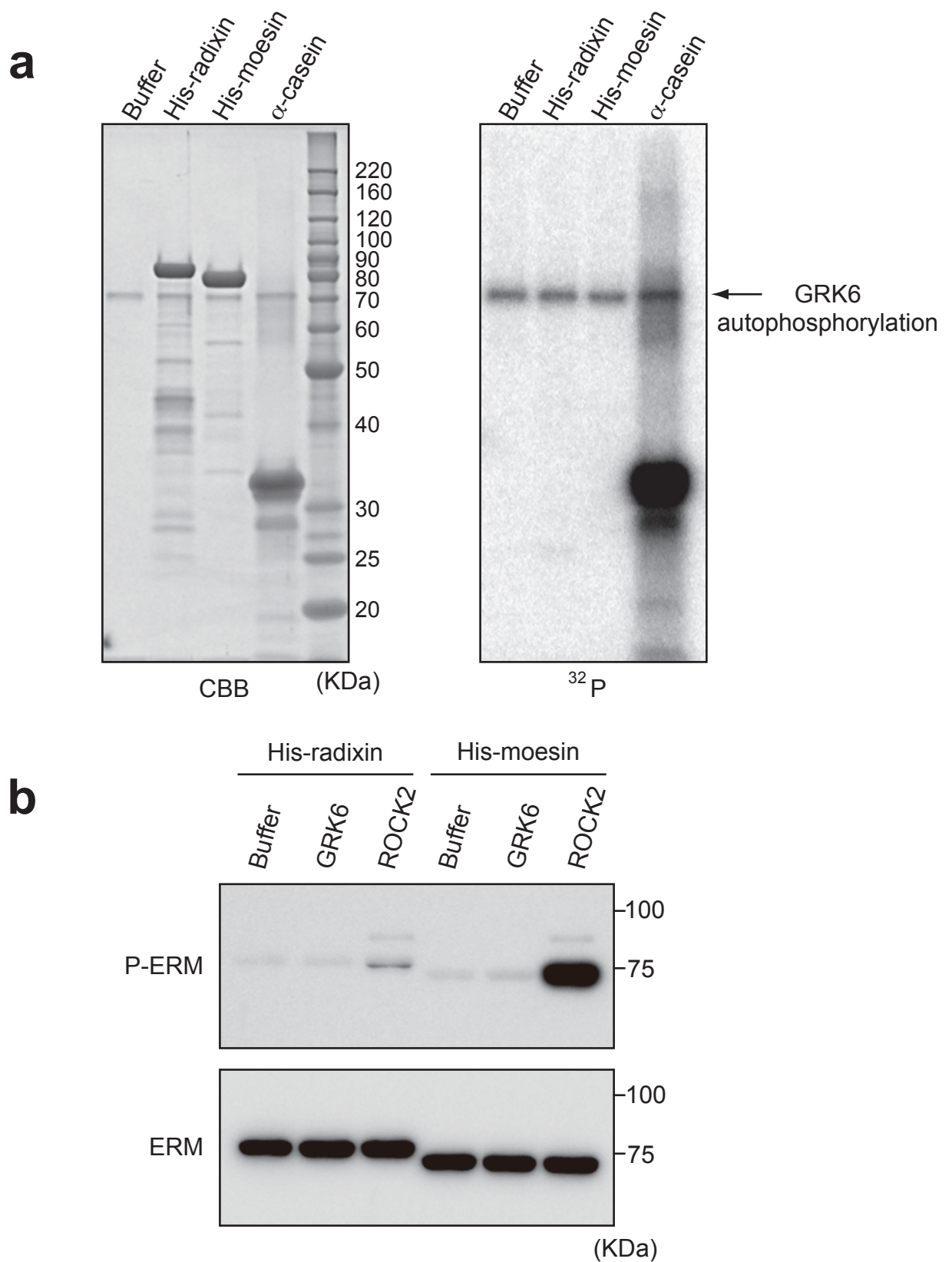


**Supplementary Fig. S9 Matching between the 2D-DIGE image and the western blot image of NIH3T3 cells overexpressing GRK6 (WT) and GRK6 (K215R)**



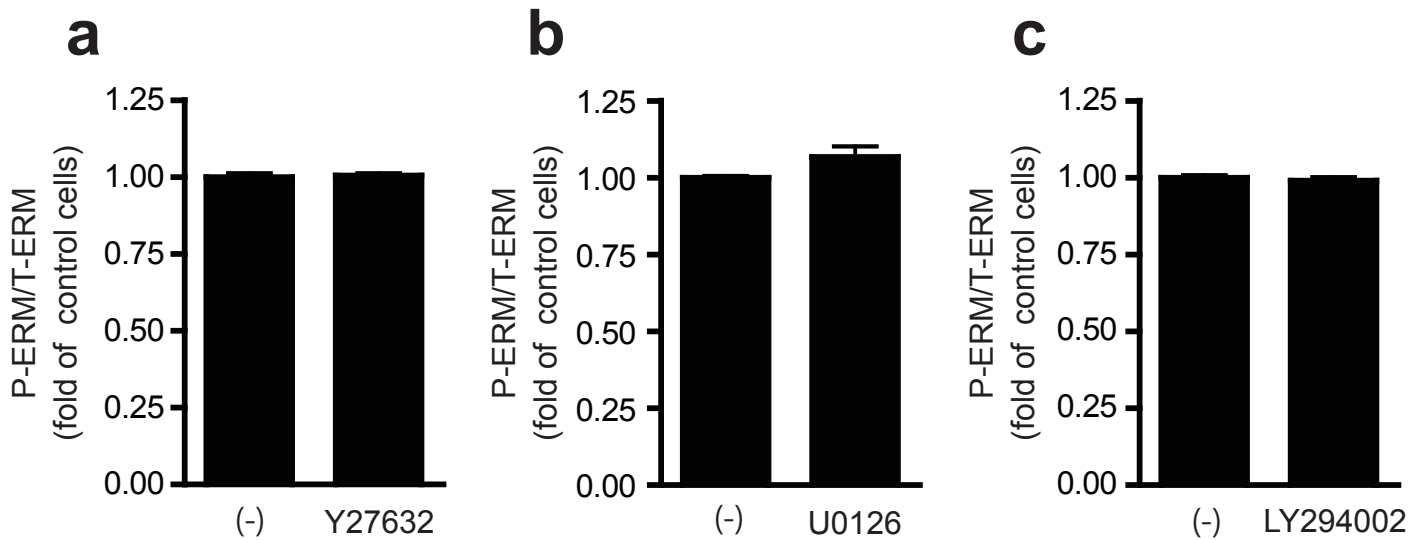
(a-c) 2D-DIGE image of samples from GRK6 (WT)-overexpressed (Cy3-labeled, red) and GRK6 (K215R)-overexpressed (Cy5-labeled, green) NIH3T3 cells (a) and western blot images from the same gel probed for anti-phospho-ERM (b) and anti-ERM (c) antibodies. The western blot signals of chemifluorescence and the Cy3- and Cy5-signals on the membrane were simultaneously detected with a fluorescence scanner. (d) The magnified views of the boxed region in (a-c) were displayed in a vertical row. The table represents protein name, reactivity to anti-phospho-ERM and anti-ERM antibodies for the numbered spots.

Supplementary Fig. S10 GRK6 does not directly phosphorylate radixin and moesin.



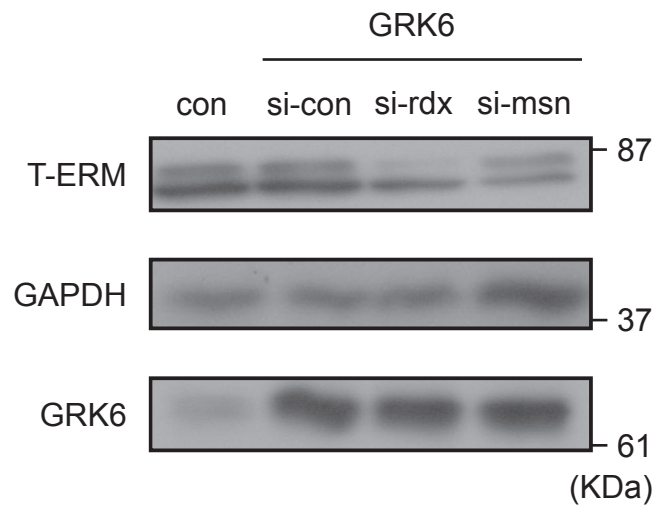
(a) Bacterially expressed His-tagged radixin and moesin were subjected to *in vitro* kinase assay with GRK6. The left gel image represents total protein stained by Coomassie Brilliant Blue, and the right gel image shows autoradiography of  $^{32}\text{P}$  labeling.  $\alpha$ -casein was used as a positive control. (b) Western blot analysis of *in vitro* phosphorylated His-radixin and His-moesin with the anti-phospho-ERM and anti-ERM antibodies. ROCK2 was used as a positive control.

**Supplementary Fig. S11 Effect of ROCK, MEK/ERK and PI3K on GRK6-induced ERM phosphorylation.**



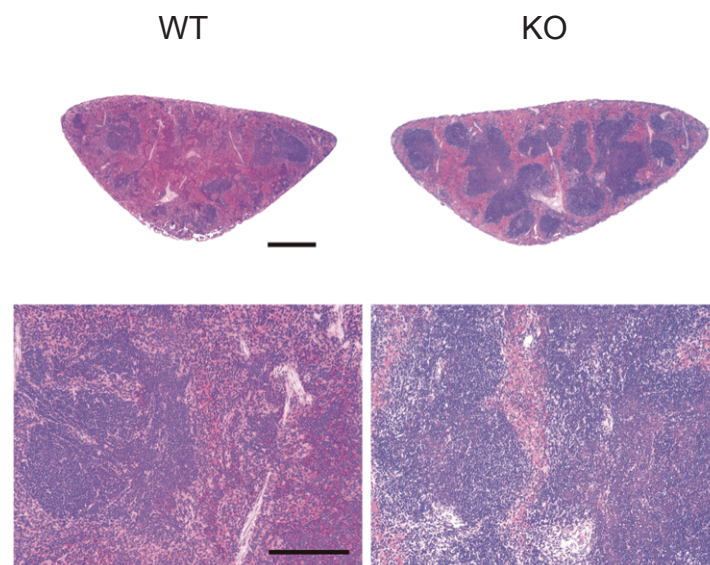
ERM phosphorylation by GRK6 was evaluated in the presence of Y27632 (30 $\mu$ M), an inhibitor of ROCK activity (**a**), U0126 (10 $\mu$ M), a MEK inhibitor (**b**) and LY242002 (10 $\mu$ M), a PI3K inhibitor (**c**). NIH3T3 cells overexpressing GRK6 were treated for the inhibitors for 1 h. The cell lysates were detected by western blot analysis with anti-phospho-ERM and anti-ERM antibodies. Data represent means  $\pm$  s.e.m. (error bars) of three independent experiments.

**Supplementary Fig. S12 The knockdown efficiency of radixin and moesin in siRNA-treated NIH3T3 cells.**



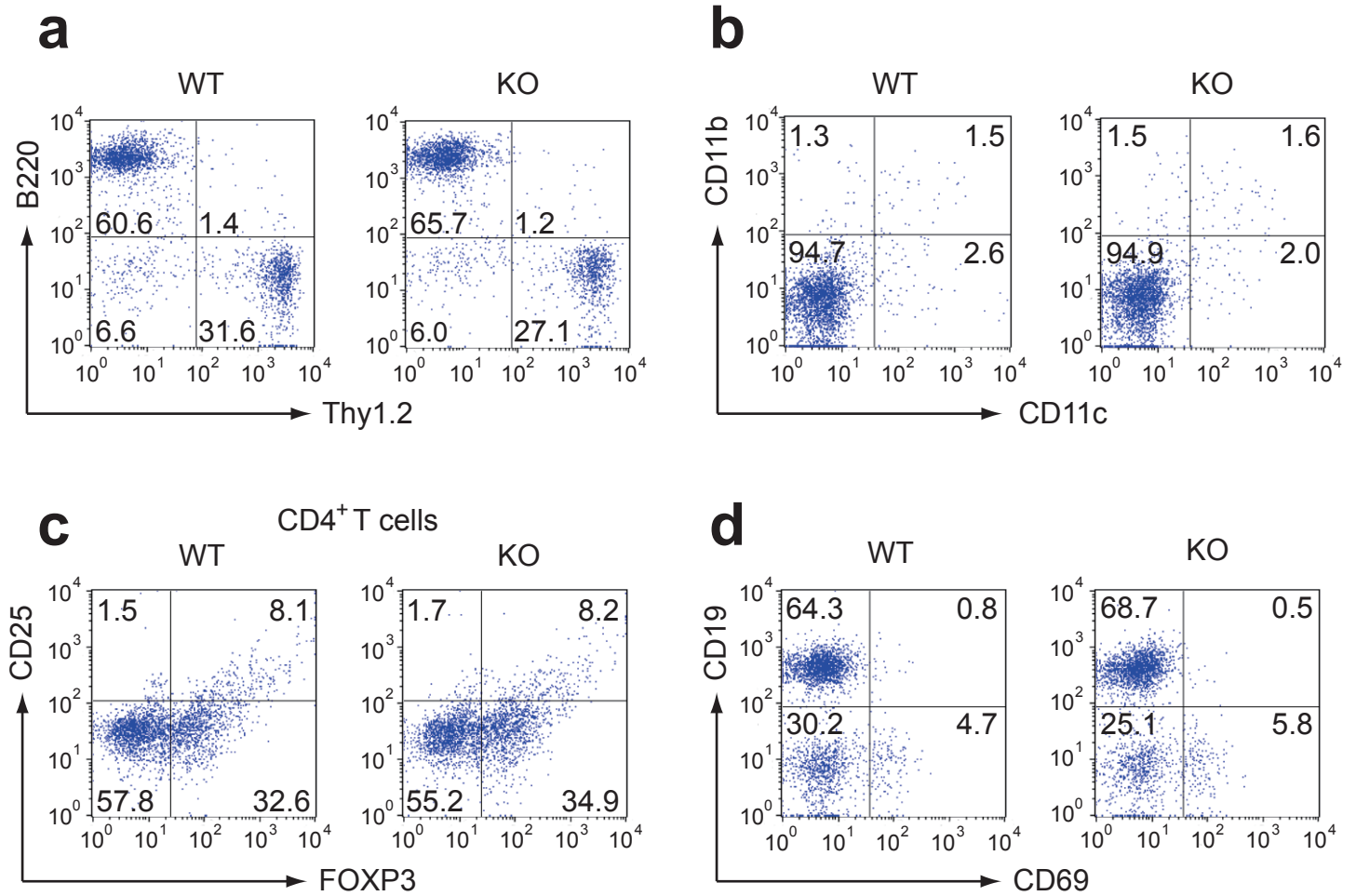
NIH3T3 cells overexpressing GRK6 were transfected with siRNA against radixin or moesin were lysed. The protein samples were analyzed by western blot using anti-ERM, anti-GRK6 and anti-GAPDH antibodies.

**Supplementary Fig. S13 Representative histology of the spleen from 40-week-old wild-type and GRK6-deficient mice.**



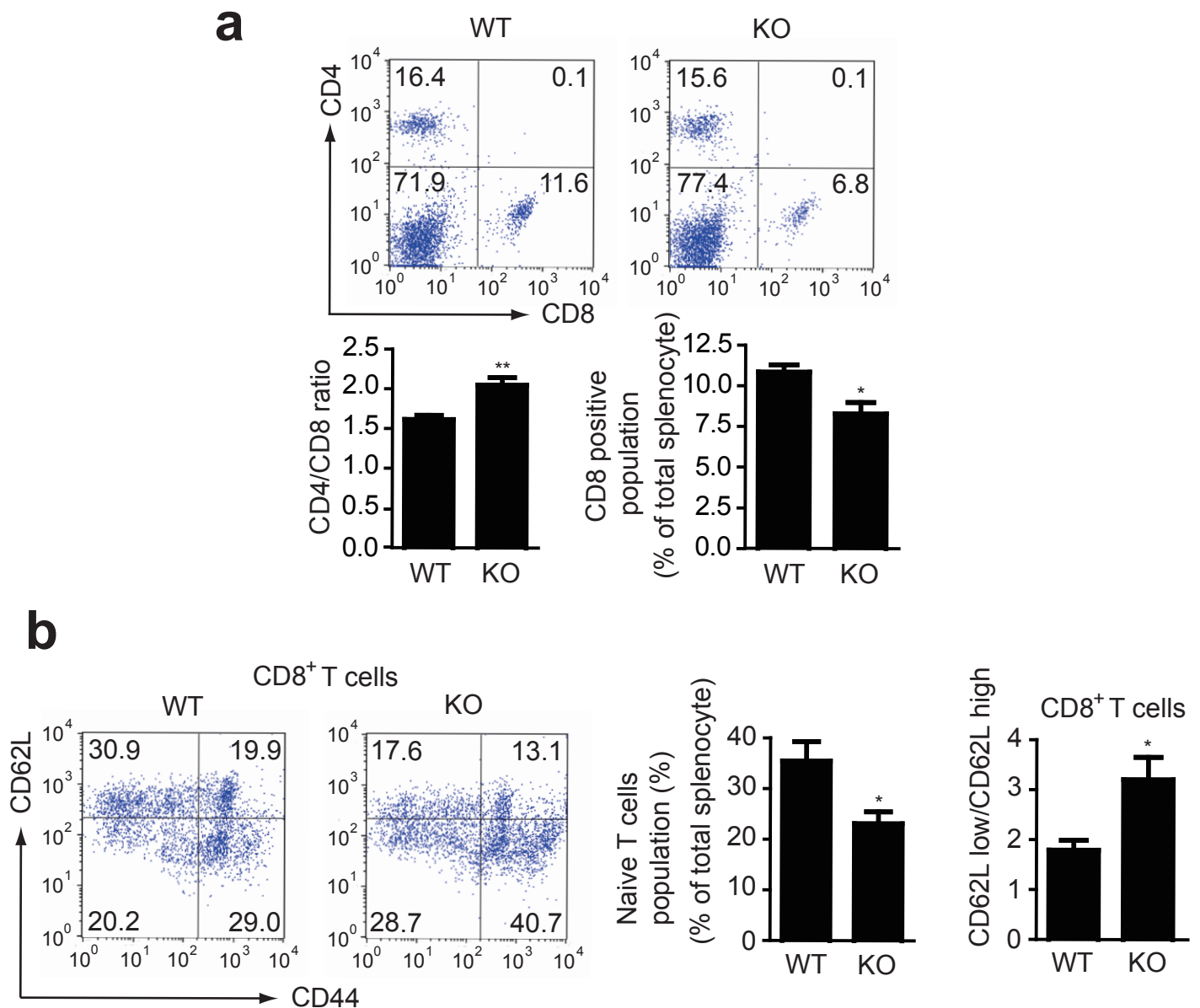
Spleen sections from 40-week-old wild-type and GRK6-deficient mice were stained with H&E. Scale bar, 300 $\mu$ m. Enlarged images are shown in the lower column. Scale bar, 100 $\mu$ m.  $n=4$ .

**Supplementary Fig. S14 Flow cytometric analysis of spleen cells from wild-type and GRK6-deficient mice at 40 weeks of age.**



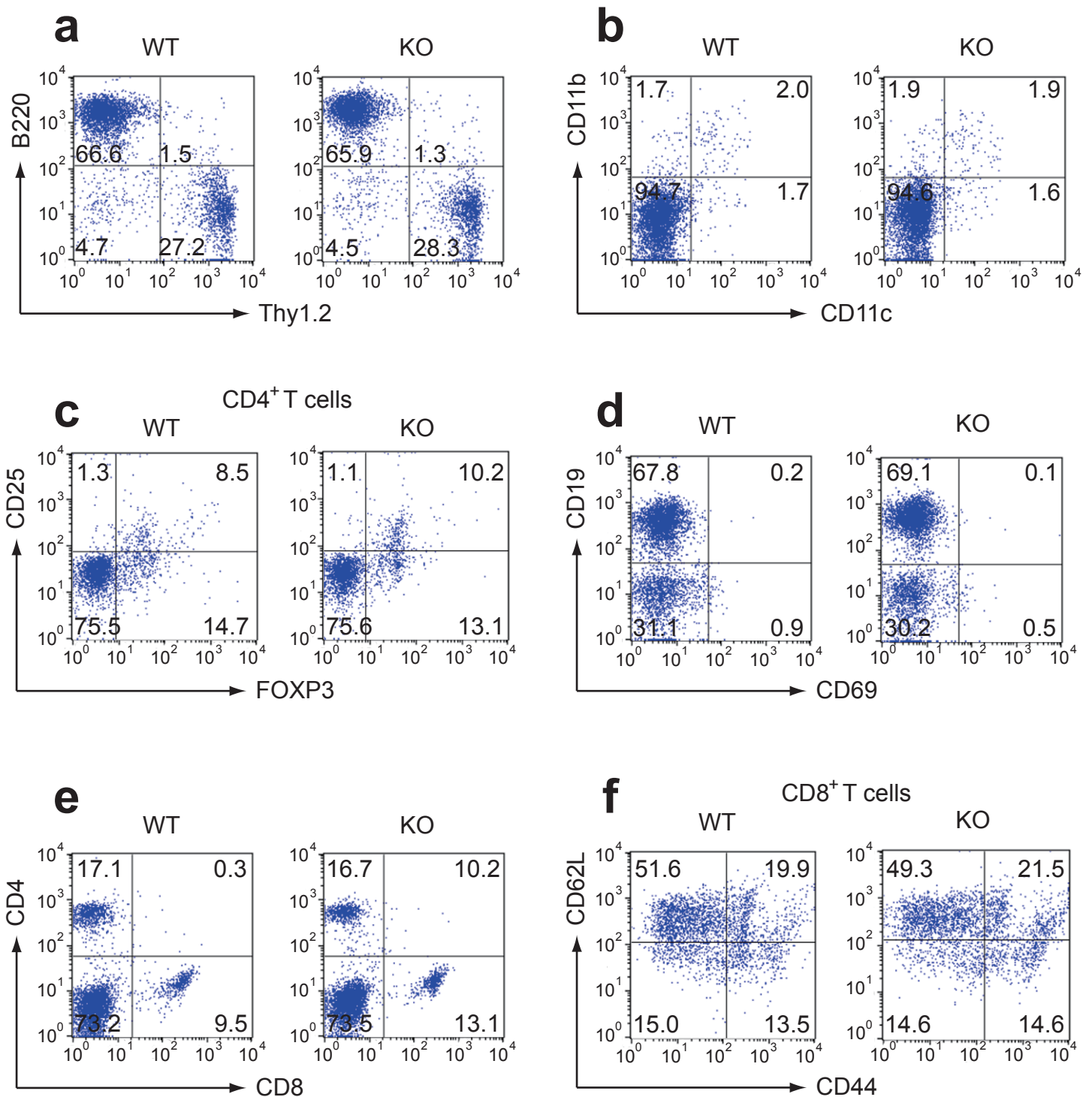
Spleens were collected from wild-type and GRK6-deficient mice of 40-week-old. The spleens were homogenized and stained with the antibodies to (a) Thy1.2 and B220 (b) CD11b and CD11c (c) CD4, CD25 and FOXP3 (d) CD69 and CD19. Data shown are representative FACS dot plots. All numbers within FACS profiles correspond to the percentage of cells within each region.  $n=4$ .

**Supplementary Fig. S15 T-cell abnormalities were observed in spleens of GRK6-deficient mice.**



(a) Isolated spleen cells from wild-type and GRK6-deficient mice of 40-week-old were stained with anti-CD4 and anti-CD8 antibodies. Numbers in quadrants indicated percent cells in each throughout. Quantitative analysis of CD4/CD8 ratio or CD8 positive population is shown right. (b) Frequency of naive CD8<sup>+</sup>T cells (CD44<sup>lo</sup> CD62L<sup>hi</sup>), central memory CD8<sup>+</sup>T cells (CD44<sup>hi</sup> CD62L<sup>hi</sup>) and effector memory CD8<sup>+</sup>T cells (CD44<sup>hi</sup> CD62L<sup>lo</sup>) among total splenocytes from wild-type and GRK6-deficient mice were analyzed by flow cytometer. Quantitative analysis of the naive CD8<sup>+</sup>T cell population or the ratio between CD62L low and CD62L high CD44<sup>+</sup>CD8<sup>+</sup> T cell population in wild-type and GRK6-deficient mice is shown (right). *n*=4. \*, *P*<0.05, \*\*, *p*<0.01. Data represent means ± s.e.m. (error bars) of four independent experiments.

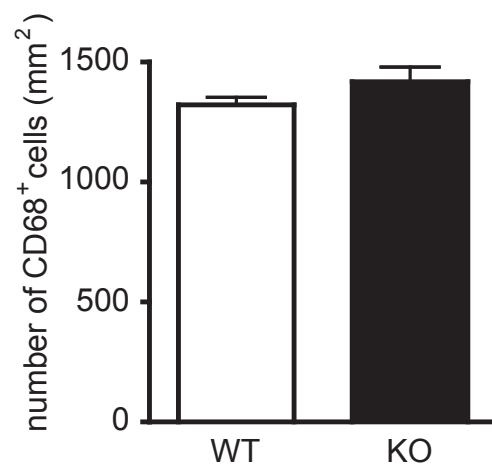
**Supplementary Fig. S16 Flow cytometric analysis of spleen cells from wild-type and GRK6-deficient mice at 8 weeks of age.**



The spleen cells from wild-type and GRK6-deficient mice of 40-week-old were stained with the antibodies to (a) Thy1.2 and B220 (b) CD11b and CD11c (c) CD4, CD25 and FOXP3 (d) CD69 and CD19 (e) CD4 and CD8 (f) CD8, CD44 and CD62L. Data shown are representative FACS dot plots. All numbers within FACS profiles correspond to the percentage of cells within each region.  $n=4$ .

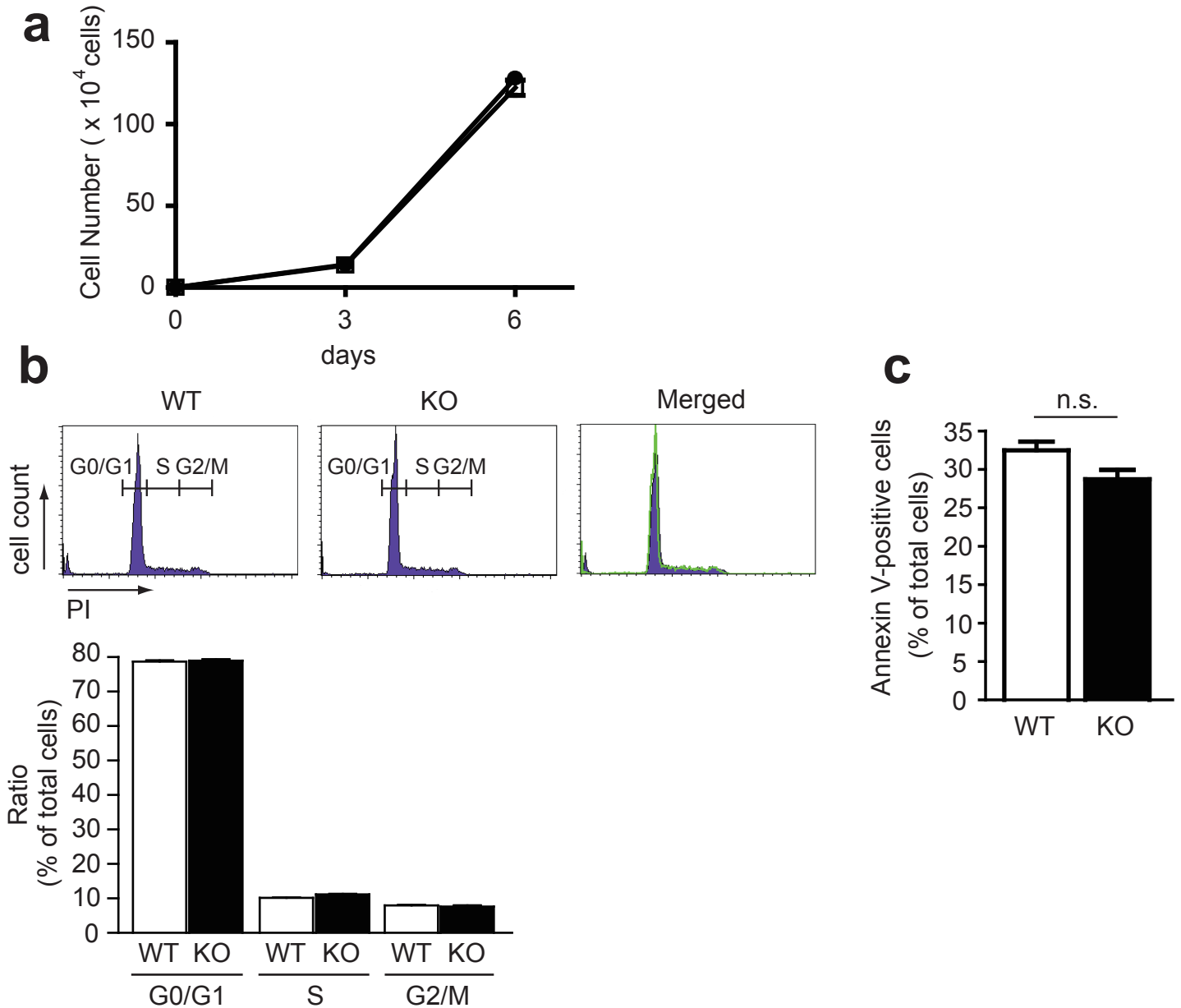


**Supplementary Fig. S17 Numbers of CD68 positive spleen cells from wild-type and GRK6-deficient mice.**



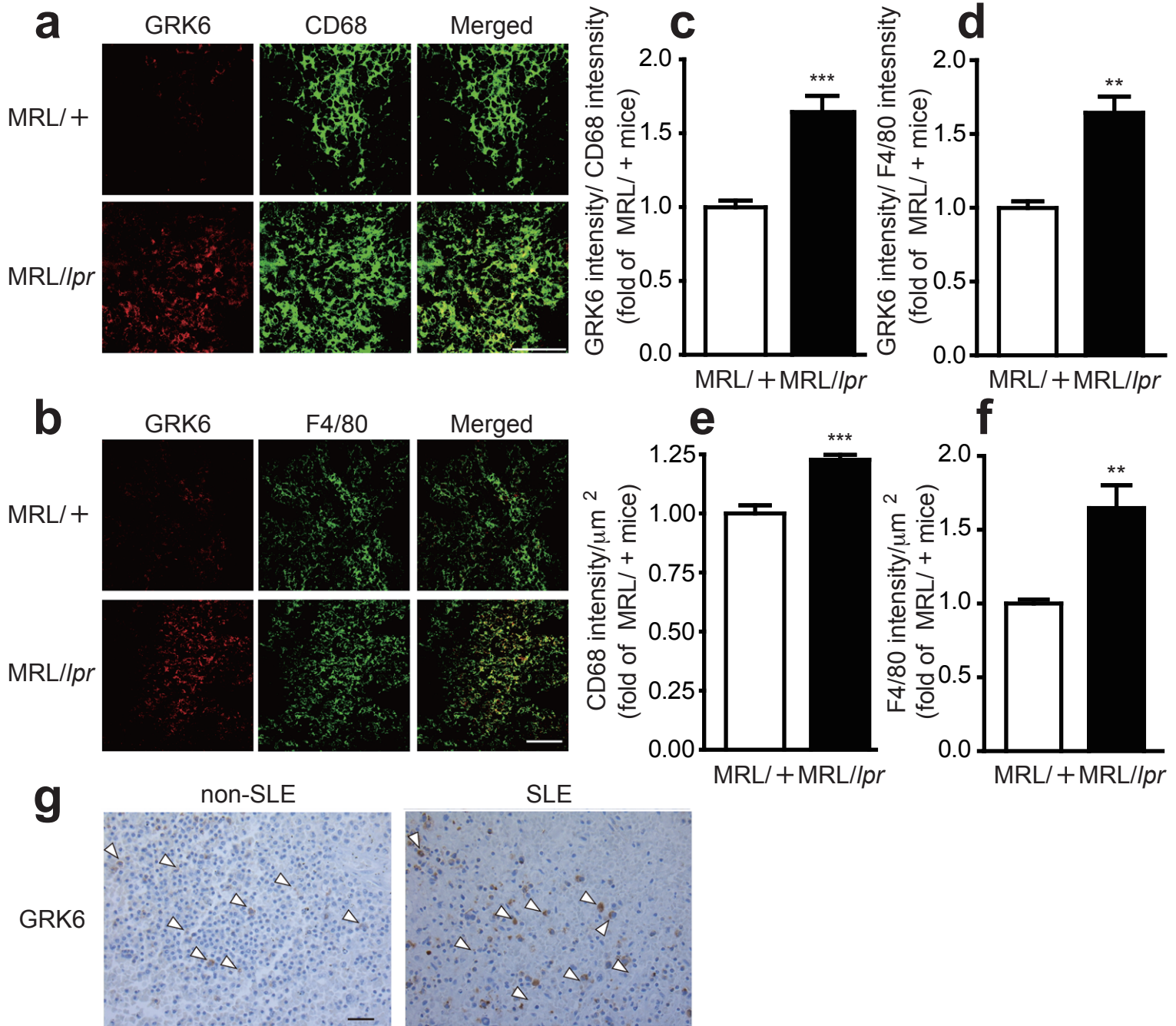
The numbers of CD68<sup>+</sup> cells were counted for at least 4 different fields (0.045 mm<sup>2</sup>) of the white pulp on each spleen section from wild-type or GRK6-deficient mice. The results are shown as mean  $\pm$  s.e.m.  $n=3$ . \*;  $P<0.05$ .

**Supplementary Fig. S18 GRK6 did not affect cell growth, cell cycle and apoptosis.**



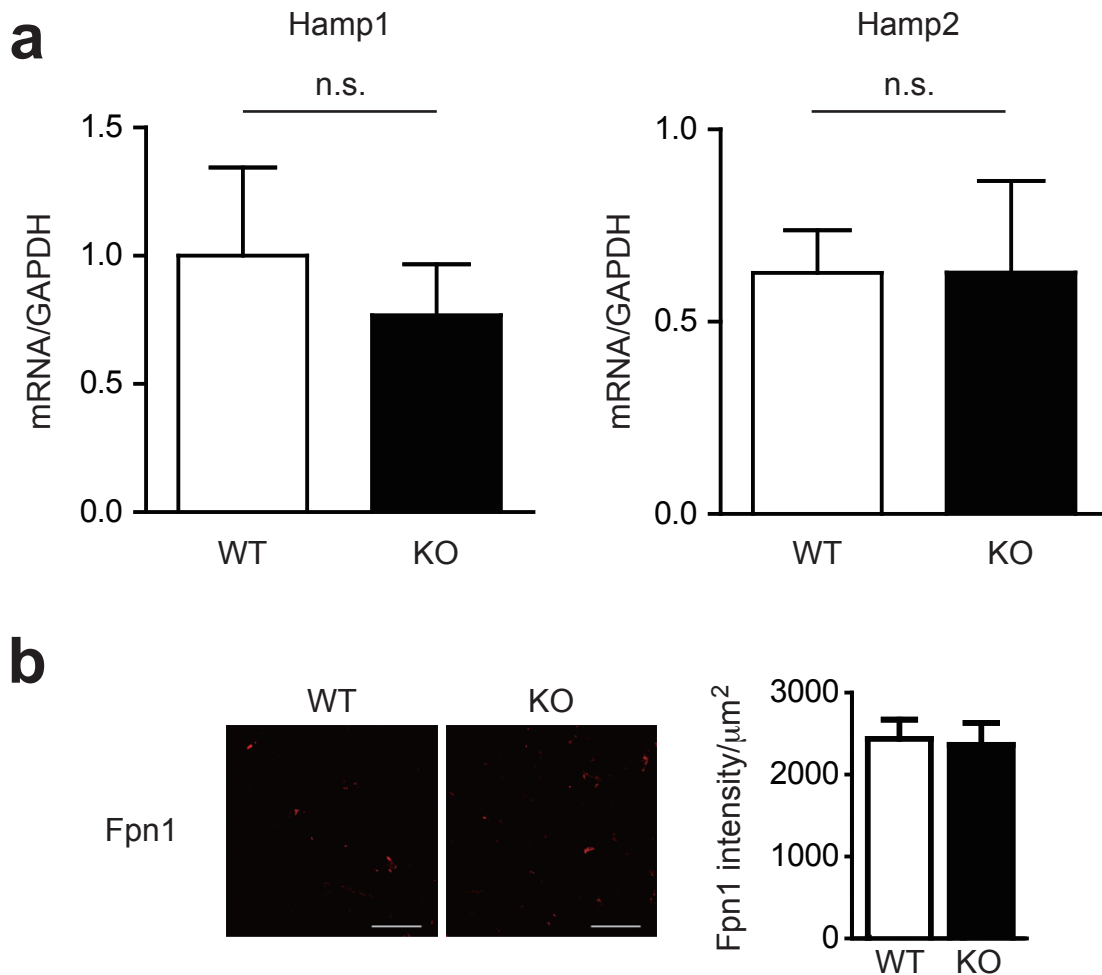
(a) Bone marrow cells isolated from wild-type or GRK6-deficient mice were cultured in the  $\alpha$ -MEM containing 10% FBS, and macrophage colony-stimulating factor on 6 cm plates ( $3 \times 10^5$  cells) and allowed to undergo differentiation. On day 3 or day 6 from the start of the culture, the number of the differentiated cells attached on each 6 cm plate was counted.  $n=4$ . (b) Cell cycle analysis of BMDM (6<sup>th</sup> day of differentiation) from wild-type or GRK6-deficient mice were performed by using a commercially available kit, whereby PI-stained nuclei were analyzed by flow cytometry. The representative FACS profiles obtained from wild-type BMDM or GRK6-deficient BMDM and overlay profiles from wild-type (purple) and GRK6-deficient BMDM (green) were shown. Gated populations in each FACS profile represent G0/G1, S and G2/M cell populations. The percentage of wild-type or GRK6-deficient BMDM in each phase of cell cycle were determined and represented in the graph.  $n=4$ . (c) BMDM (6<sup>th</sup> day of differentiation) from wild-type or GRK6-deficient mice were treated with LPS (100 ng/ml) to undergo apoptosis at 37 °C for 2 h. After the treatment, BMDM were stained with Annexin V-GFP. The percentages of Annexin V-positive cells were assessed. n.s.; not significant.  $n=4$ . Data represent means  $\pm$  s.e.m.

**Supplementary Fig. S19 GRK6 expression is increased in splenic macrophages of MRL/lpr mice and a SLE patient.**



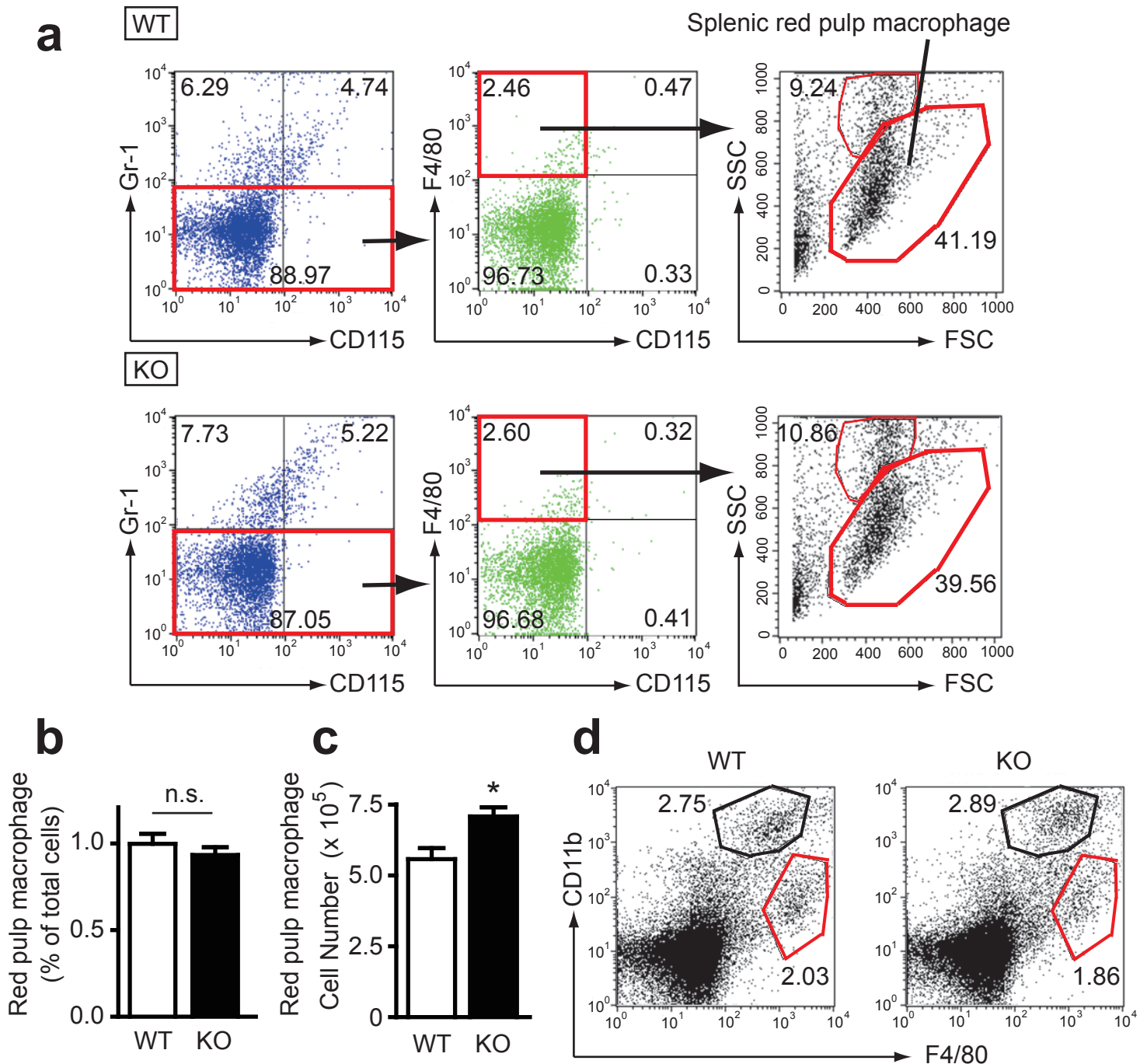
(a, b) Spleen sections from MRL/lpr and from its control, MRL/+ mice were stained with anti-GRK6 (red) and (a) anti-CD68 (green) or (b) anti-F4/80 (green) antibodies. Scale bar, 50  $\mu\text{m}$ . (c, d) The expression level of GRK6 in splenic macrophages was determined as the ratio of GRK6 intensity to (c) CD68 intensity or (d) F4/80 intensity in 5-6 areas. The fold increases were calculated by the values of MRL/+ set as 1.  $n=3$ . (e, f) The number of (e) CD68 or (f) F4/80 positive macrophages was increased in MRL/lpr mice. The fold increases were calculated by the values of MRL/+ set as 1.  $n=3$ . (g) Hematoxylin and eosin (H&E) staining of lymph node sections. Splens from patients with systemic lupus erythematosus (SLE) and controls without SLE (non-SLE controls) were formalin fixed and paraffin embedded. The sections stained with hematoxylin were evaluated for GRK6 expression by immunohistochemistry. Arrowheads indicate inflammatory cells expressing GRK6. Scale bar, 20  $\mu\text{m}$ . \*\*,  $p<0.01$ , \*\*\*,  $P<0.001$ . Data represent means  $\pm$  s.e.m.

**Supplementary Fig. S20 Hamp1 and Hamp2 expression in spleen, Ferroportin1 expression in liver of GRK6-deficient mice.**



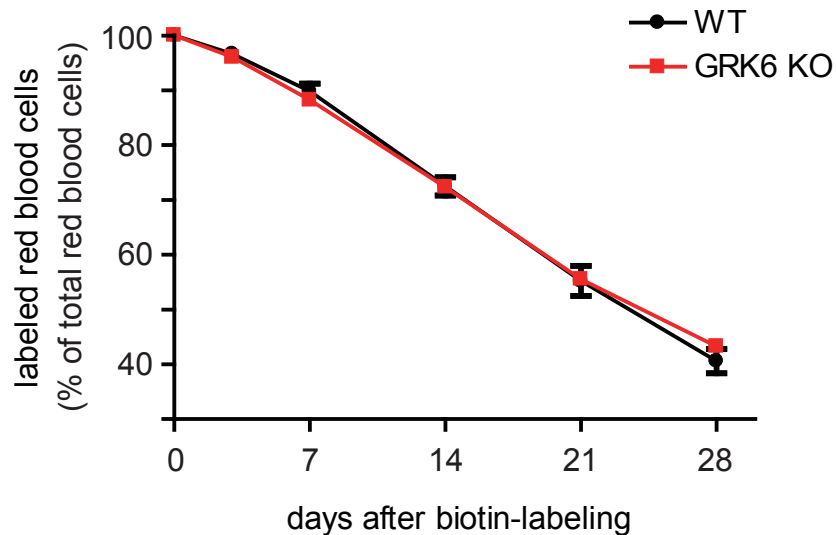
(a) mRNA expression levels of Hamp1 and Hamp2 genes in wild-type and GRK6-deficient spleens. Total RNAs were extracted from spleens of wild-type and GRK6-deficient mice (Spleen extirpation was performed twenty-four hours after the last bleeding). The expression levels of Hamp1 and Hamp2 mRNA were evaluated by real-time RT-PCR. The fold increases were calculated by the values of wild-type mice at steady state set as 1.  $n=3-5$ . (b) Liver sections from wild-type or GRK6-deficient mice were stained with anti-Fpn1 antibody. Intensity of Fpn1-immunoreactive signals was evaluated.  $n=4$ . Scale bar, 50  $\mu\text{m}$ . #;  $P<0.05$ . Data represent means  $\pm$  s.e.m.

**Supplementary Fig. S21 Flow cytometric analysis of splenic red pulp macrophages from wild-type and GRK6-deficient mice**



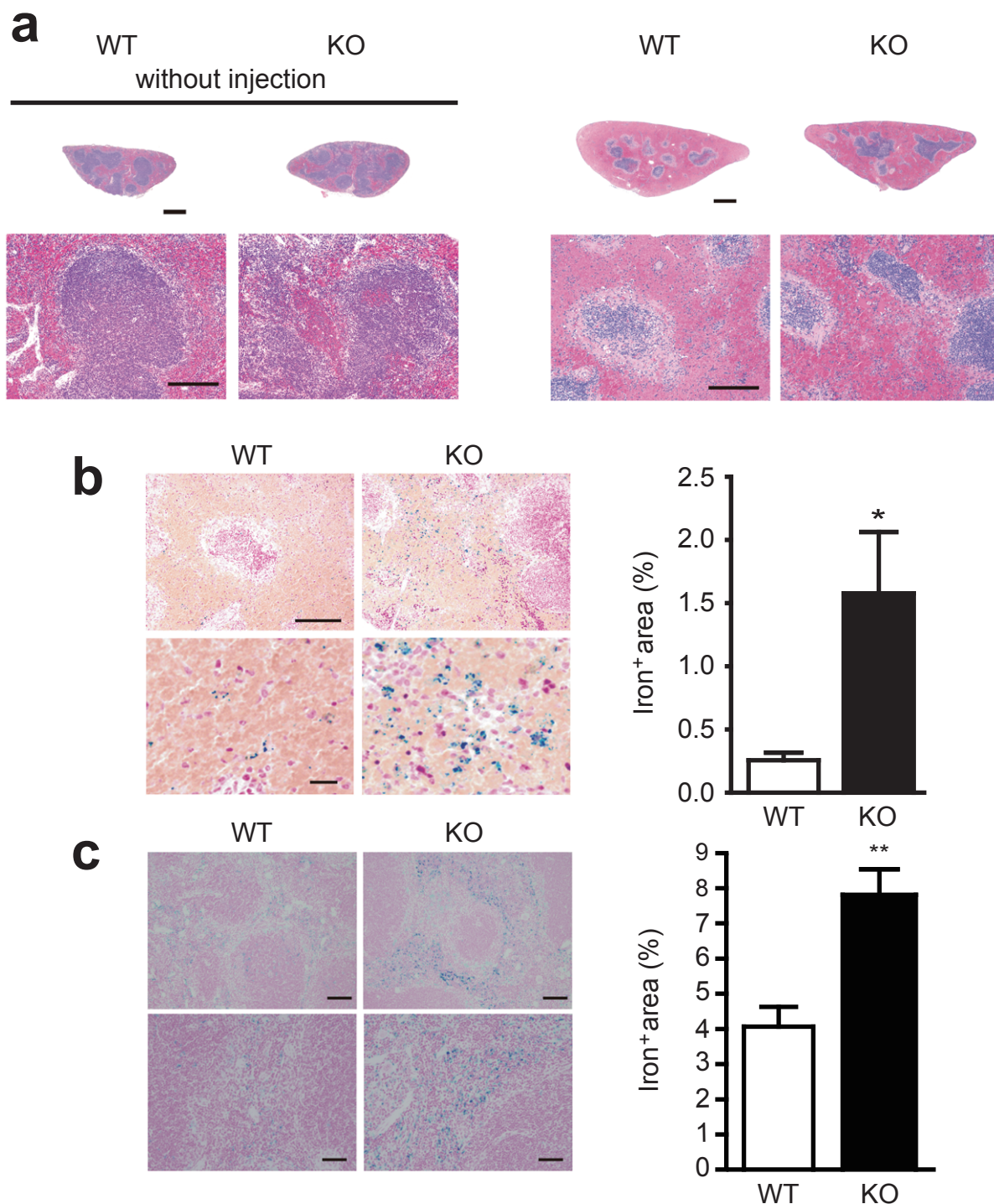
(a) Splenocytes isolated from wild-type or GRK6-deficient mice were stained with anti-Gr-1-FITC, anti-CD115-APC, and anti-F4/80-PerCP/Cy5.5 antibodies. Splenic red pulp macrophage population was defined as Gr-1<sup>lo</sup> CD115<sup>lo</sup> F4/80<sup>+</sup> SSC<sup>int/lo</sup> cells. Representative FACS profiles are shown. All numbers within FACS profiles correspond to the percentage of cells within each region. (b, c) The relative (b) and absolute (c) numbers of splenic red pulp macrophages are shown. Data represent means  $\pm$  s.e.m. of three independent experiments. (d) The expressions of F4/80 and CD11b on splenocytes from wild-type or GRK6-deficient mice were determined by flow cytometer. Numbers indicate the percentages of F4/80<sup>hi</sup>CD11b<sup>lo</sup> macrophages (red lines) or F4/80<sup>+</sup>CD11b<sup>hi</sup> (black lines) monocyte/macrophages. Similar percentages of F4/80<sup>hi</sup>CD11b<sup>lo</sup> macrophages and F4/80<sup>+</sup>CD11b<sup>hi</sup> were seen between wild-type and GRK6-deficient splenocytes. Representative FACS dot plots are shown.  $n=4$ .

**Supplementary Fig. S22 Erythrocyte life span in wild-type and GRK6-deficient mice.**



Erythrocytes in wild-type and GRK6-deficient mice ( $n=5-6$  in each group) were biotinylated by tail vein injection of EZ-Link Sulfo-NHS-biotin and blood was drawn every week. Erythrocytes isolated were incubated with phycoerythrin-conjugated streptavidin and biotinylated erythrocytes were quantified by flow cytometry. Values represent the mean  $\pm$  s.e.m. of mice ( $n=5-6$ ). Ratio of biotinylated erythrocytes at the indicated time points was evaluated. The ratio of biotinylated erythrocytes at the starting point was set to 100%.

**Supplementary Fig. S23 Iron deposition in the spleen from wild-type and GRK6-deficient mice after anemia.**



(a) Mice were injected with 0.15 mg/g body weight of phenylhydrazine. Twenty-four hours after the injection, their spleens were isolated. Spleen sections from phenylhydrazine-injected wild-type ( $n=10$ ) and GRK6-deficient mice ( $n=7$ ) were stained with H&E. Scale bar, 300  $\mu\text{m}$ . Enlarged images are shown in the lower column. Scale bar, 100  $\mu\text{m}$ . Spleen sections from wild-type and GRK6-deficient mice without phenylhydrazine injection were also stained with H&E. (b) Spleen sections from phenylhydrazine-injected 10-week-old wild-type and GRK6-deficient mice were subjected to Perl's Prussian blue staining. Scale bar, 100 $\mu\text{m}$ . Enlarged images were shown directly below the originals. Scale bar, 10 $\mu\text{m}$ . Areas staining positive for iron were quantified with BZ-II Analyzer software, and shown as a percentage of the total surface area. The average numbers are shown with S.D.  $n=3$ . (c) Spleen sections from 10-week-old wild-type and GRK6-deficient mice treated with phlebotomy were subjected to Perl's Prussian blue staining. Scale bar, 100  $\mu\text{m}$ . Enlarged images were shown directly below the originals. Scale bar, 50  $\mu\text{m}$ . Areas staining positive for iron were quantified as described in (b).  $n=3$ . \*,  $P<0.05$ , \*\*,  $P<0.01$ . Data represent means  $\pm$  s.e.m.

**Supplementary Table. S1 Serum parameters of 2-month-old wild-type and GRK6-deficient mice.**

4-month-old-mice

	WT (n=18)	KO (n=9)	P
Serum iron ( $\mu\text{g/dL}$ )	178 $\pm$ 10	164 $\pm$ 8.1	0.38
UIBC ( $\mu\text{g/dL}$ )	236 $\pm$ 7.4	223 $\pm$ 7.7	0.29
TIBC ( $\mu\text{g/dL}$ )	414 $\pm$ 11	387 $\pm$ 11	0.14
TS (%)	43 $\pm$ 1.7	42 $\pm$ 1.5	0.87

The sample size (n) is indicated. Serum iron parameters in 2-month-old (WT, 7 male, 11 female; GRK6-deficient mice, 3 male, 6 female) are shown. UIBC or TIBC indicates unsaturated iron binding capacity or total iron-binding capacity respectively; TS represents transferrin saturation. Data are mean  $\pm$  s.e.m. P represents the value of a Student t-test.



**Supplementary Table. S2 Serum parameters of 10-month-old wild-type and GRK6-deficient mice.**

10-month-old-mice

	WT (n=11)	KO (n=8)	P
Serum iron ( $\mu\text{g/dL}$ )	152 $\pm$ 14	123 $\pm$ 11	0.14
UIBC ( $\mu\text{g/dL}$ )	212 $\pm$ 8.4	238 $\pm$ 25	0.28
TIBC ( $\mu\text{g/dL}$ )	364 $\pm$ 7.2	362 $\pm$ 19	0.87
TS (%)	41 $\pm$ 2.8	35 $\pm$ 3.7	0.18

The sample size (n) is indicated. Serum iron parameters in 4-month-old (WT, 7 male, 11 female; GRK6-deficient mice, 3 male, 6 female) and 10-month-old (WT, 11 female; GRK6-deficient mice, 8 female) are shown. Data are mean  $\pm$  s.e.m. P represents the value of a Student t-test.

## Supplementary Methods

**Mice.** GRK6-deficient mice (backcrossed for more than 12 generations on the C57BL/6 background) or MFG-E8-deficient mice (C57BL/6 × 129Sv background) were obtained from Drs. R. J. Lefkowitz and R. T. Premont (Duke University) or Dr. S. Nagata (Kyoto University), respectively. Mice were age- and sex-matched and kept under pathogen-free conditions in accordance with Institutional Animal Care and Use committee regulations. All experiments using mice and rats were approved by the guidelines of Kyushu University. MRL/MP-lpr/lpr (MRL/lpr) mice and MRL/MP-+/+(MRL/+) mice were purchased from SLC (Japan).

**Cell culture and transfection.** A retrovirus-packaging cell line, PLAT-E cell<sup>48</sup>, NIH3T3 cell, and HEK293 cell were cultured in DMEM containing 10% fetal bovine serum (FBS) and 1% penicillin/streptomycin solution. Preparation of bone marrow-derived macrophages (BMDM) were described previously<sup>21</sup>, and they were maintained in the  $\alpha$ -MEM medium containing 10% FBS and macrophage colony-stimulating factor (M-CSF) that is prepared from the conditioned medium of L929 cells transformed with a human M-CSF expression plasmid<sup>49</sup>. HEK293 cells and PLAT-E cells were transfected with Fugene 6 reagent (Roche). Lipofectamine 2000 (Invitrogen) was used for siRNA transfection. Retrovirus infection of NIH3T3 cells using the culture supernatant of PLAT-E cell was performed as described previously<sup>21</sup>. In brief, objective genes were inserted into pMXs-puro retrovirus vector. Plasmid DNA carrying each gene was introduced by lipofection using Fugene 6 (promega) into PLAT-E cells. Two days after transfection, the culture supernatant containing each retrovirus was collected and added on NIH3T3 cells in the presence of polybrene (10

μg/ml) (Sigma).

**Reagents.** A MEK inhibitor, U0126 was purchased from Sigma. A Rho-kinase inhibitor, Y-27632 was obtained from WAKO (Japan). A PI3K inhibitor, LY294002 was purchased from Calbiochem.

**Plasmids constructs and siRNA.** Mouse GRKs (GRK2, 3, 5 and 6), Rac1, ELMO1/2, GULP, and GIT1 were amplified from thioglycollate-elicited mouse peritoneal macrophage cDNA library. The cDNAs were subcloned into pMXs-puro and fused with an N-terminal Flag tag. Kinase-inactive form of each GRK [GRK2 (K220R), GRK3 (K220R), GRK5 (K215R), and GRK6 (K215R)] and dominant negative form of Rac1, Rac1 (T17N) were generated by site-directed mutagenesis using QuickChange mutagenesis kit (Stratagene). Various deletion mutants of GIT1, a dominant negative form of GULP, GULP (PTB), and dominant negative forms of ELMO, ELMO1 (T625) and ELMO2 (T615) were also made by the mutagenesis kit. GRK6 or GIT1 were tagged with Flag or HA and inserted into pcDNA3 vector for immunoprecipitation assay. All the validated siRNAs were purchased from Invitrogen. The target sequences for mouse GRK6 was 5'-AAUAAACAGGCGCCCAAUGGGCUGGC-3', for mouse radixin was 5'-UUCGCAUGUACAGUUCAUGGUUCC-3', for mouse moesin was 5'-AGUAAAUGUCGUCAUUGAGAAUGCC-3', for mouse GRK2 was 5'-GGCAGCGGCGAUACUUCUACUUGUU-3'. As a control, stealth RNAi siRNA negative controls (Invitrogen) were used in each experiment. NIH3T3 cells were transfected with siRNAs by Lipofectamine 2000 (Invitrogen).

**Phalloidin staining.** NIH3T3 cells infected with the empty retrovirus vector or with vectors expressing GRK6, GRK6 (K215R), Rac1, Rac1 (T17N) were plated on the glass-bottom base dishes coated by poly-L-Lysine. On the next day, the cells were washed by PBS and 4% paraformaldehyde was treated for 15 min at room temperature to fix them. After the fixation, the cells were washed by PBS again, and permeabilized with 0.1% Triton X-100 for 5 min followed by PBS wash. The cells were then blocked with 1% BSA in PBS solution. After removing the blocking solution, the cells were incubated with Alexa 568-phalloidin solution for 40 min. The images for the cells were obtained by confocal microscope (Zeiss, LSM510-META).

**Preparation of recombinant proteins.** The open reading frame of mouse radixin or moesin was ligated into pCold II vector (TAKARA) for its bacterial expression as a 6x-histidine (His) tagged fusion protein. Mouse GIT1 cDNA was inserted into pCold II vector with N-terminal GST-tag. His-radixin, His-moesin or GST-GIT1 was expressed in *Escherichia coli* strain BL21 (DE3) cultured with 500  $\mu$ M isopropyl- $\beta$ -D-thiogalactopyranoside at 15 °C for 24 h. The bacteria were centrifuged and removed the supernatant. The bacterial pellets were freeze-thawed 3 times and then suspended in a lysis buffer (50 mM Tris-Cl, 500 mM NaCl, 10% glycerol, 1% Triton X-100, pH8.0 at 4 °C) containing 1 mg/ml Lysozyme and protease inhibitor cocktail (Nacalai). The suspension was incubated for 30 min and sonicated followed by centrifugation (4,620 x g for 20 min) at 4 °C. His-radixin or His-moesin in the supernatant was purified by a Ni-NTA His bind Resin (Novagen). GST-GIT1 was purified by a column packed with glutathione-sepharose beads (GE Healthcare). The His-tagged proteins were eluted with elution buffer (50 mM Tris-Cl, 100 mM NaCl,

10% glycerol, 250 mM imidazole, pH 8.0 at 4 °C). GST-GIT1 was eluted with the buffer (100 mM Tris-Cl, 20 mM glutathione, pH 8.0 at 4 °C). The eluted proteins were dialyzed for 24 h at 4 °C against repeated changes of dialysis buffer (10 mM Tris-Cl, 150 mM NaCl, 1 mM dithiothreitol, 0.1% Tween 20).

***In vitro* kinase assay.** Baculovirus-expressed recombinant full-length GRK6 (Carna Biosciences) (200 ng) was incubated with His-radixin (5 µg), His-moesin (5 µg), GST-GIT1 (3.5 µg) or  $\alpha$ -casein (5 µg) (Sigma) and 100 µM [ $\gamma$ -<sup>32</sup>P] ATP (5.0 µCi) in 20 µl kinase buffer (20 mM Tris-HCl, pH 7.5, 5 mM MgCl<sub>2</sub>, and 1 mM DTT) for 30 min at 30 °C. The reaction was stopped by adding Laemmli's sample buffer and boiling. The samples were then subjected to SDS-PAGE and the phosphorylation level of each substrate was estimated by autoradiography of the gel.

**Western blot analysis.** Samples from lysed cells or tissues (5 µg total protein) were subjected to western blotting and detected with anti-GRK2 (1:2,000, Santacruz), anti-GIT1 (1:2,000, Santacruz), anti-phospho-MEK1 (Ser298) (1:2,000, CST), anti-MEK1 (1:2,000, CST), anti-phospho-ERK1/2 (Thr202/Tyr204) (1:5,000, CST), anti-phospho-PAK1 (Thr423) (1:2,000, CST), anti-PAK1/2/3 (1:5,000, CST), anti-phospho-Akt (Ser473) (1:2,000, CST), anti-Akt (1:5,000, CST), anti-ERM antibody (1:2,000, CST), anti-phospho ERM antibody (1:2,000, CST) or anti-GAPDH antibodies (1:5,000, Santacruz), followed by either anti-rabbit IgG or anti-mouse IgG secondary antibodies conjugated to horseradish peroxidase at a dilution of 1:4,000 (Santacruz) and detection using the ECL System (PerkinElmer).

**2-D Western blot analysis.** Two-dimensional western blot analysis was carried out as described previously<sup>28</sup>. In brief, phosphoprotein-enriched fractions prepared from NIH3T3 cells overexpressing GRK6 or GRK6 (K215R) were labeled by Cy3 or Cy5 respectively. Then the fractions were rehydrated into pH 3–10 immobilized pH gradient strips (24cm) followed by isoelectric focusing, resolved by 9% SDS-PAGE, and transferred to a polyvinylidene difluoride membrane. Immunoblotting was performed using the anti-phospho-ERM antibody or anti-ERM antibody with chemiluminescent and chemifluorescent detection by ECL Plus reagent (GE Healthcare).

**Flow cytometry.** Whole splenocytes and lymph nodes were depleted of erythrocytes by using Red Blood Cell Lysis Buffer (Roche) and stained with anti-B220-allophycocyanin (APC), anti-Thy1.2-FITC, anti-CD11b-APC, anti-CD11c-FITC, anti-CD8-FITC, anti-CD4-PerCP/Cy5.5, anti-CD19-APC, anti-CD8-PerCP/Cy5.5, anti-CD44-FITC, anti-CD62L-APC, anti-CD25-APC, anti-FOXP3-Alexa488, anti-Gr-1-FITC, anti-F4/80-PerCP/Cy5.5, anti-CD115-APC and anti-F4/80-FITC. The antibodies were purchased from Biolegend. The stained cells were analyzed by a FACS Calibur.

**Real-time RT-PCR.** Total RNA was isolated from spleens of mice using Isogen (Nippongene) according to the manufacturer's instructions and treated with RNase-free DNase I (Qiagen). RNA concentration and purity were assessed by spectrophotometry (Thermoscientific). mRNA expression was quantified by real-time RT-PCR using TaqMan probes. The obtained results were normalized to GAPDH. TaqMan probes for were purchased from Applied Biosystems.

Primers used for real-time RT-PCR.

Gene	Primer
<i>gapdh</i>	Forward: 5'- TGCCCCCATGTTTGTGATG -3' Reverse: 5'- GGCATGGACTGTGGTCATGA -3' probe: 5'- ACCACCAACTGCTTAGCCCCCCTG -3'
<i>hamp1</i>	Assay ID: Mm04231240_s1 (Applied Biosystems)
<i>hamp2</i>	Assay ID: Mm00842044_g1 (Applied Biosystems)

**Evaluation of cell growth, cell cycle and apoptosis.** Bone marrow cells were collected from a 20-week-old female wild-type or GRK6-deficient mice. The collected cells were treated with Red Blood Cell Lysis Buffer (Roche). After the treatment, the cells were suspended in  $\alpha$ -MEM (GIBCO) containing 10% FBS and M-CSF. The cell count was adjusted to  $1.0 \times 10^5$  cells/ml for the cell growth experiment, and the cells were plated on 6 cm plates. Three days and 6 days after the seeding, the cells were detached from the plates, and the number of the cells on plates was counted. For the experiment of cell cycle and apoptosis analysis, the count of bone marrow cells were adjusted to  $1.0 \times 10^6$  cells/ml and the cells were cultured on 10 cm plates. Three days after, the differentiating cells attached on the plates were collected and re-seeded at  $1.0 \times 10^5$  cells/ml. Six days after the start of the culture, we collected the differentiated macrophages and performed cell cycle analysis of the macrophages using Cycletest Plus DNA Reagent Kit according to the manufacture's protocol (BD Biosciences), followed by FACS analysis. The macrophages were also treated with LPS (100 ng/ml) to undergo apoptosis at 37 °C for 2 h. The treated macrophages were incubated with AnnexinV-GFP (1:100 dilution, MBL) for 30 min at room temperature in the AnnexinV binding buffer (10 mM HEPES-OH, 140 mM NaCl, 2.5 mM CaCl<sub>2</sub>, pH 7.5), followed by FACS analysis.

**Determination of serum iron parameters.** Quantification of serum iron concentration and unsaturated iron binding capacity (UIBC) was measured by a chelating agent 2-nitro-S-(N-propyl-N-sulfopropylamine) phenol (Quick Auto Neo Fe, Shino-Test Co., Tokyo, Japan). An automatic analyzer (Model 7180 Automatic Analyzer Hitachi High-technologies Corporation) was used for the measurement.

**Anemia induction.** Anemia was induced by phenylhydrazine hydrochloride (0.15 mg/g body weight) (Sigma) administration or phlebotomy (16  $\mu$ l/g body weight, twice for 24 h). Phenylhydrazine hydrochloride was dissolved in sterile phosphate-buffered saline and pH of the solution was adjusted to 7.4. The phenylhydrazine hydrochloride solution was freshly prepared and administered to age-matched adult male mice by intraperitoneal injection.

**Immunohistochemistry.** Cryosections (4  $\mu$ m) of the spleen of MRL/*lpr* mice or MRL/+ mice were fixed in cold-acetone for 10 min. After the fixation, the sections were blocked with PBS containing 3% BSA for 1hr, and subsequently incubated with anti-GRK6 (1:50 dilution, Santacruz), anti-CD68 (1:200 dilution, Serotec), or anti-F4/80 (1:200 dilution, Serotec) overnight at 4 °C, followed by staining with fluorescent conjugated secondary antibodies.

Among 1528 autopsy cases performed in department of pathology at Tokyo Medical University during 1994-2011, 6 women cases were diagnosed as SLE. The slides of the paraffin-embedded spleen of the SLE patients were stained by anti-GRK6 antibody (1:1,000 dilution, Santacruz). For the antigen retrieval, deparaffinized slides were autoclaved in Tris-EDTA solution (10 mM Tris-Base, 1 mM EDTA, pH 9.0) at 121 °C



for 10 min before the staining. All the stained sections were observed under a fluorescence microscope (Keyence BZ-9000) or a confocal microscope (Olympus FV10i or Nikon A1Rsi).

**Determination of red blood cell life span.** *In vivo* biotinylation of red blood cells was performed as previously reported<sup>50</sup> with some modifications. In brief, EZ-Link NHS-LC-Biotin (Thermo scientific) was dissolved in PBS and adjusted to 5 mg/ml. 150  $\mu$ l of the biotin solution was injected into wild-type or GRK6-deficient mice. Two hours after the injection, about 5  $\mu$ l of their blood was collected and stained with streptavidin-PE (1:500 dilution; Biolegend) for 30 min at 4°C. The red blood cells were subjected to FACS analysis to confirm that the biotinylation efficiency of the cells was more than 98%. Seven, 14, 21 or 28 days after the biotin labeling, red blood cells was collected from the mice, and the percentage of the biotin-labeled red blood cells in mice was determined.

### Supplementary References

- 48 Morita, S., Kojima, T. & Kitamura, T. Plat-E: an efficient and stable system for transient packaging of retroviruses. *Gene Ther.* **7**, 1063-1066 (2000).
- 49 Takeshita, S., Kaji, K. & Kudo, A. Identification and characterization of the new osteoclast progenitor with macrophage phenotypes being able to differentiate into mature osteoclasts. *J. Bone Miner. Res.* **15**, 1477-1488 (2000).
- 50 Suzuki, T. & Dale, G. L. Biotinylated erythrocytes: *in vivo* survival and *in vitro* recovery. *Blood* **70**, 791-795 (1987).